Estimation of the period of free oscillations (seiches) in the Kirrbucht

OCEANOLOGIA, No. 38 (4)
pp. 505–528, 1996.
PL ISSN 0078–3234

Kirrbucht
Seiches
Numerical modelling

Kurt Frischmuth
Department of Mathematics,
Rostock University,
Rostock

Andrzej Jankowski
Institute of Oceanology,
Polish Academy of Sciences,
Sopot

Manuscript received July 15, 1996, in final form September 18, 1996.

Abstract

An attempt was made to estimate the periods of the main seiches in the Kirrbucht, a shallow water basin with an irregular coastline. A quasi-linear hydrodynamic-numerical model of the storm surges (wind-driven circulation) in a shallow density-homogeneous basin was used. The results of calculations of sea level oscillations generated in the basin in response to a temporally and spatially constant wind field (stress) were treated as a time series in order that the seiche periods could be calculated. The standard discrete Fourier transformation was applied to estimate amplitude spectra. The periods of the three significant modes were found to be equal to 3.21 min, 4.94 min and 6.59 min. The latter two are probably fundamental ones: they are the transverse and longitudinal modes respectively. The influence of non-linear terms and lateral fricton on the seiche periods is also discussed.

1. Introduction

Wind impulses generate periodic water movements which, when the wind suddenly stops blowing or rapidly changes direction and/or velocity, take the form of seiches – free periodic oscillations or normal modes (Proudman, 1953; Defant, 1961; Fairbridge, 1966). Their characteristic periods and phases depend on the principal characteristics of the water basin, *i.e.* its bottom topography and its morphometry (shoreline shape). These phenomena can be observed in time series of different, measurable *in situ* hydrophysical parameters, *e.g.* current velocity components, sea level or temperature. Thus

a knowledge of the periods (and phases) of the seiches allows the free oscillations to be distinguished from other phenomena. If necessary they should be filtered from the data, so that the time variability of the processes under investigation can be estimated more accurately.

The period of a seiche is readily estimated in a basin with a straightforward shape from Merian's formulae (Proudman, 1953; Defant, 1961; Fairbridge, 1966; Druet, 1978):

– in the case of a narrow elongated enclosed basin with a flat bottom topography:

$$T_{sn} = \frac{2L}{n\sqrt{(gH_0)}}, \tag{1}$$

where

T_{sn} – period of n-th order seiche (n – mode of free oscillations),
$n = (1, 2, 3,...)$ – integers, defining the harmonic modes (or number of nodes) of the seiche,
L, H_0 – the characteristic horizontal dimension and the characteristic depth of the water basin,
g – acceleration due to gravity,
$\sqrt{(gH_0)}$ – phase velocity of the long, non-dispersive waves;

– in the case of a 2D rectangular enclosed basin with a flat bottom topography:

$$T_{sn} = \frac{2}{\sqrt{(gH_0)}} \left(\frac{m^2}{L_x^2} + \frac{n^2}{L_y^2} \right)^{-1/2}, \tag{2}$$

where

$m, n = (1, 2, 3,...)$ – integers defining the coexisting harmonic modes or the number of nodes in the transverse and longitudinal directions,
L_x, L_y, H_0 – characteristic horizontal dimensions of the rectangular basin: length (L_x), breadth (L_y), in x and y directions and the characteristic (or mean) depth of the water basin (mean) respectively,
g – acceleration due to gravity,
$\sqrt{(gH_0)}$ – phase velocity of the long, non-dispersive waves.

The periods and amplitudes of the seiches can be estimated by means of an analysis of the *in situ* time series of standard hydrological parameters (current components, sea level, temperature *etc.*). In order to discover more detailed characteristics of the space-time structure of the seiches, mathematical modelling is applied (*cf.* Krauss, 1973; Druet, 1978, for more information). Where a water basin has a more irregular shoreline and/or a more

complex bottom topography, more complicated physical and mathematical models, equations and methods have to be applied (*cf. e.g.* Hollan, 1983).

In this paper we propose a simple method of estimating the periods of the main harmonic modes of the free oscillations. The idea is based on the application of the results of a hydrodynamic-numerical model, of the type used to calculate storm surges, wind-driven circulation *etc.* (*cf.* Simons, 1973; Ramming and Kowalik, 1980; Kowalik and Murty, 1993). More precisely, the model involves a time series of sea level oscillations generated during numerical calculations at each grid point which are then used to detect the periodic structure of the oscillations by means of standard time series analysis *i.e.* the Discrete Fourier Transformation (DFT) (Bendat and Piersol, 1986). A similar approach was used by Lewandowicz and Staśkiewicz (1983) with respect to Puck Bay.

The principal objective of this paper is to apply the method to discover the periods of the free oscillations in a shallow basin with an irregular shoreline: the Kirrbucht is a good example of this kind of water basin.

Located in the southern Baltic off north-eastern Germany (Fig. 1), the Kirrbucht is a very small shallow water basin (maximum bottom depth < 13 m) with an indented shoreline (Fig. 2). The dynamics of the water in

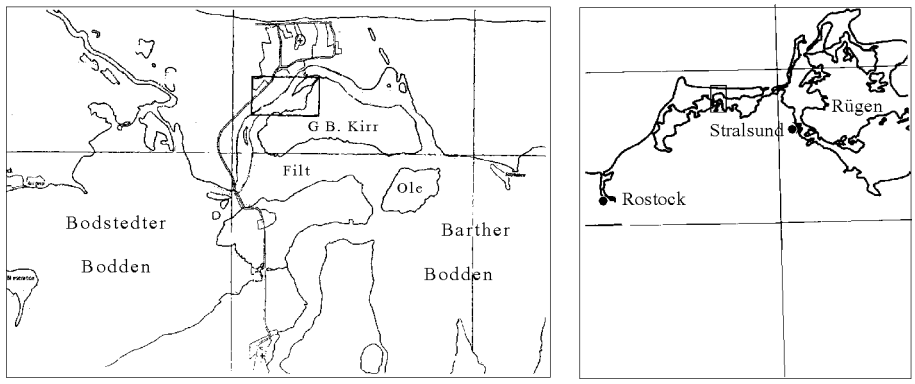

Fig. 1. Location of the Kirrbucht and the adjacent basins

this shallow basin are believed to be mainly of the wind-driven type and play an important role in the formation of the hydrological background for the marine environment. Owing to the lack of *in situ* measurements to estimate the water dynamics, numerical modelling is the simplest way of estimating some basic features of the water movements or assessing the orders of magnitude of the temporal and spatial scales of variability in the hydrophysical

(dynamic) parameters. Some of these time scales are periods of free oscillations that can be easily estimated *en passant* during the calculation of storm surges or the water circulation with the aid of hydrodynamic-numerical models.

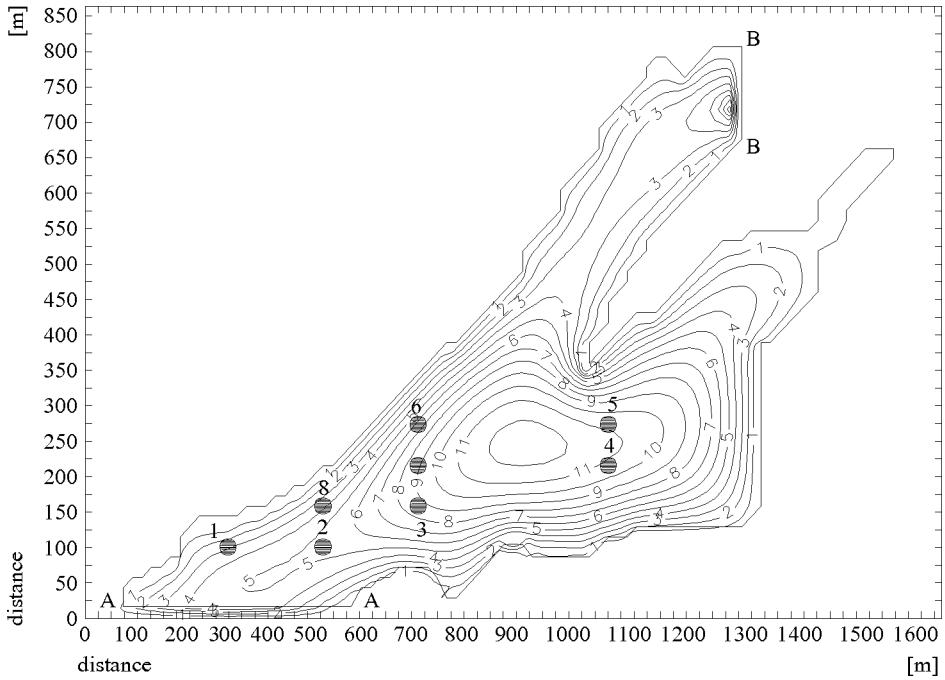

Fig. 2. Bottom topography [m] of the Kirrbucht used in the model. The numbered dots indicate the points on the numerical grid at which the time series of sea level fluctuations were used in calculations. Lines A–A and B–B indicate the connections of the Kirrbucht with adjacent basins

Because of the small size of the Kirrbucht and its shallow depth, it can be assumed that the water density is homogeneous and that the water movements in the closed basin are generated mainly by wind stress.

The calculations were carried out for southerly and westerly winds blowing with a constant velocity of 8 m s^{-1} in order to estimate the longitudinal and the transverse seiche modes.[1] The influence of lateral friction and non-linear terms in the equations of motion on seiche periods is also discussed.

[1]The longitudinal and transverse seiche modes are here regarded as the y-axis and the x-axis seiche modes respectively.

2. Model equations

In order to estimate the general features of the water dynamics the Hansen hydrodynamic-numerical model (Hansen, 1962; Ramming and Kowalik, 1980) was used. This kind of model has been found useful in the calculation of storm surges, tides and currents in a variety of seawater bodies.

The model is based on the following set of equations of motion and the continuity equation describing 2D water dynamics in shallow seawater basins of homogeneous density (*cf.* Simons, 1973; Ramming and Kowalik, 1980; Kowalik and Murty, 1993):

$$\frac{\partial M_x}{\partial t} + \underline{\frac{\partial}{\partial x}\left(\frac{M_x M_x}{H}\right) + \frac{\partial}{\partial y}\left(\frac{M_x M_y}{H}\right)} - f M_y = $$

$$= -H\frac{\partial p_a}{\partial x} - \rho_0 g H \frac{\partial \zeta}{\partial x} + \tau_x^s - \tau_x^b + \underline{\underline{A_l \triangle M_x}}, \tag{3}$$

$$\frac{\partial M_y}{\partial t} + \underline{\frac{\partial}{\partial x}\left(\frac{M_x M_y}{H}\right) + \frac{\partial}{\partial y}\left(\frac{M_y M_y}{H}\right)} + f M_x = $$

$$= -H\frac{\partial p_a}{\partial y} - \rho_0 g H \frac{\partial \zeta}{\partial y} + \tau_y^s - \tau_y^b + \underline{\underline{A_l \triangle M_y}}, \tag{4}$$

$$\frac{\partial \zeta}{\partial t} + \frac{1}{\rho_0}\left(\frac{\partial M_x}{\partial x} + \frac{\partial M_y}{\partial y}\right) = 0. \tag{5}$$

The initial conditions for eqs. (3)–(5) can be written in the following form:

$$\text{for} \quad t = 0, \qquad \zeta = 0, \qquad M_x = 0, \qquad M_y = 0. \tag{6}$$

The lateral boundary conditions take the form:

$$M_n = \begin{cases} 0 & \text{at the solid (closed) boundary,} \\ \Phi(L) & \text{at the liquid (open) boundary,} \end{cases} \tag{7}$$

$$M_\tau = \begin{cases} 0 & \text{at the solid (closed) boundary,} \\ \Phi 1(L) & \text{at the liquid (open) boundary,} \end{cases} \tag{8}$$

where

$$M_x = \int_{-\zeta}^{H_o} \rho_0 u dz, \qquad M_y = \int_{-\zeta}^{H_o} \rho_0 v dz,$$

where

$M_x,\ M_y$ – x- and y-mass transport components along the OX and OY axes,

$u,\ v$ – current velocity vector components along the OX, OY axes respectively,

A_l – lateral eddy viscosity coefficient (assumed constant),
$f = 2\,\omega \sin\varphi$ – Coriolis parameter ($\omega = 0.729 \times 10^{-5}$ rad s^{-1} – angular velocity of the Earth's rotation about its own axis; φ – latitude),
ρ_0 – seawater density (assumed constant),
g – acceleration due to gravity,
$\tau_x^s,\ \tau_y^s$ – tangential wind stress components at the free sea surface,
$\tau_x^b,\ \tau_y^b$ – tangential water shear stress components at the sea bottom,
ζ – sea level (ordinate of free sea surface),
$\triangle = \frac{\partial^2}{\partial x^2} + \frac{\partial^2}{\partial x^2}$ – horizontal Laplace operator,
p_a – atmospheric pressure (assumed constant),
t – time,
H_o – undisturbed water basin depth,
$H = H_o + \zeta$ – total water basin depth,
$M_n,\ M_\tau$ – mass transport vector components, normal and tangential to the lateral boundary L respectively,
$\Phi(L),\ \Phi 1(L)$ – functions describing the water balance at the open sea boundary (*i.e.* river mouth or link with adjacent sea area).

The tangential wind stress components τ_x^s, τ_y^s, and the tangential bottom water stress components τ_x^b, τ_y^b, were calculated by means of the well-tried formulae used in hydrodynamic-numerical models (Simons, 1973; Ramming and Kowalik, 1980; Jankowski, 1988; Kowalik and Murty 1993):

– wind stress components:

$$\tau_x^s = \rho_a C_D W_a W_x, \qquad \tau_y^s = \rho_a C_D W_a W_y, \tag{9}$$

– bottom shear water stress components:

$$\tau_x^b = RM_x, \qquad \tau_y^b = RM_y, \qquad R = \frac{r}{H^2}\sqrt{M_x^2 + M_y^2}, \tag{10}$$

where
$W_a = \sqrt{W_x^2 + W_y^2}$ – absolute wind vector velocity,
$W_x,\ W_y$ – components of the wind vector velocity,
$\rho_a,\ C_D$ – air density and drag coefficient respectively,
r – bottom friction coefficient.

In our calculations the standard values for the air density $\rho_a = 1.3 \times 10^{-3}$ g cm^{-3}, the drag coefficient $C_D = 2.6 \times 10^{-3}$ and the bottom friction coefficient $r = 2.5 \times 10^{-3}$ usually used in calculations of storm surges and water circulation in natural basins (Simons, 1973; Ramming and Kowalik, 1980) were applied.

The main purpose of this paper was to apply the quasi-linear hydrodynamic-numerical model to estimate the periods of the fundamental seiche

modes. In order to assess the role of nonlinearity of the equations of motion and lateral eddy exchange on seiche periods, the non-linear terms (the terms underlined once in eqs. (3)–(5)) and those with the lateral viscosity (the terms underlined twice in eqs. (3)–(5)) were taken into account during the calculations.

The coefficient of the lateral turbulent exchange of momentum (lateral eddy viscosity, friction coefficient) A_l is dependent on the spatial and temporal scales of the dynamic processes and in general satisfies the Richardson law (*cf.* Defant, 1961; Ozmidov, 1968)

$$A_l = c_0 L^{4/3}, \tag{11}$$

where L denotes the horizontal scale of the turbulent eddies, an empirical constant of proportionality with an order of magnitude of 0.01 $\mathrm{cm}^{2/3}\ \mathrm{s}^{-1}$ (*cf.* Ozmidov, 1968).

In practical numerical calculations some values of the lateral eddy friction coefficient A_l were used to perform the tests and select a value which is physically and numerically appropriate to the sought-after solution. From the physical point of view the influence of lateral friction in a small and shallow water basin is minimal compared to bottom friction. However, because of the irregularities of both bottom and shoreline, the lateral friction terms can be included in the numerical model, where they are treated as smoothing terms in order to filter out the parasite instabilties generated during numerical computations due to the above-mentioned irregularities. In our model we used the latter approach when carrying out the calculations for selected values of the order of A_l (0, 10^1, 10^2, 10^3, 10^4 [$\mathrm{cm}^2\ \mathrm{s}^{-1}$]).

The underlined terms in eqs. (3)–(5) were rejected from the calculations in some experiments for the quasi-linear case and in the experiments where lateral friction was absent.

The mass transport and sea level eqs. (3)–(5) were solved by numerical methods. The explicit numerical scheme of Hansen's hydrodynamic-numerical method (Hansen, 1962; Ramming and Kowalik, 1980) was used. The finite difference forms of eqs. (3)–(5) are described in the appendix.

3. Results and discussion

The calculations were performed for winds blowing from the south and from the west with a constant velocity of 8 m s^{-1} (S 8 m s^{-1} and W 8 m s^{-1} respectively) on the assumption that the Kirrbucht is a closed basin, filled with water of homogeneous density. The connections of the Kirrbucht with adjacent basins (depicted in Fig. 2 by lines A–A and B–B) were neglected in all the results reported here. The grid space steps of the numerical grid were as follows: $h_x = 9.10$ m, $h_y = 7.20$ m and the time step, estimated according to the stability criterion (appendix, eq. (19)) was $\tau = 0.5$ s.

The duration of the calculations in each of the numerical experiments performed was 20 h.

Some runs were carried out with a time impulse of forcing – *i.e.* after 1, 5 and 10 h of simulation time the wind stress and the bottom shear stress components were put equal to zero (ceasing of forcing functions and that of describing energy dissipation in the model) to discover the response of the basin and to generate free flow conditions. The results referring to the periods recorded on the spectra were almost identical, both for short wind impulses and for those of 10 h duration; it is the latter that are reported in the present paper.

The time series of the sea level oscillations during computations were registered at 8 points in the Kirrbucht area (see Fig. 2 for location of the points). Example 'time series' of sea level variations generated during the numerical calculations at point 1 are shown in Fig. 3 for the W 8 m s^{-1} wind for the quasi-linear case and without lateral friction.

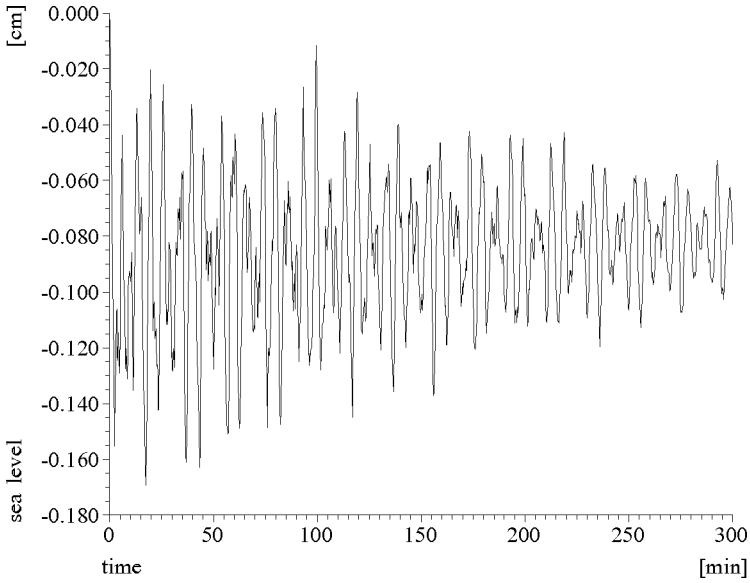

Fig. 3. Example of a time series of sea level oscillations [cm] generated by the hydrodynamic-numerical model at point 1 (for point location – see Fig. 2) for the quasi-linear case and with the lateral eddy viscosity coefficient $A_l = 0$ cm^2 s^{-1} for a W 8 m s^{-1} wind

The discrete Fourier transformation (Bendat and Piersol, 1986) was applied to each 'time series' of the sea level fluctuations registered at all 8 points.

Fig. 4 presents the amplitude spectra for the time series derived from calculations recorded at point 1 for both wind directions for the quasi-linear case (the case without non-linear terms in the equations of motion (3)–(5)) and with $A_l = 0$ cm^2 s^{-1}.

Table 1. Values of amplitudes and phases of the main seiches at 8 selected points estimated by the model for the case of a W 8 m s^{-1} wind when the lateral eddy exchange coefficient $A_l = 0$ cm^2 s^{-1} (quasi-linear case). Location of points – see Fig. 2

Point number	Seiche period [min]	Amplitude A_n [cm]	Relative amplitude A_n / A_{max}	Phase [grad]
1	3.2086	0.004604	0.0905	145.7
	4.9383	0.050867	1.0000	357.4
	6.5934	0.015343	0.3016	10.3
2	3.2000	0.000466	0.0168	34.4
	4.9383	0.027843	1.0000	357.5
	6.5934	0.011491	0.4127	10.8
3	3.2086	0.003071	0.4179	331.7
	4.9383	0.006179	0.8408	358.2
	6.5934	0.007349	1.0000	11.6
4	3.2086	0.003222	0.4674	331.3
	4.9383	0.004362	0.6328	358.3
	6.5934	0.006893	1.0000	11.6
5	3.2172	0.000394	0.0127	84.8
	4.9383	0.031004	1.0000	357.5
	6.5934	0.012070	0.3893	10.6
6	3.2086	0.002956	0.3793	332.0
	4.9383	0.007794	1.0000	358.2
	6.5934	0.007746	0.9939	11.6
7	3.2086	0.001237	0.0994	330.0
	4.9383	0.012452	1.0000	176.4
	6.5934	0.005619	0.4513	13.8
8	3.2086	0.001098	0.0858	329.3
	4.9383	0.012796	1.0000	176.5
	6.5934	0.005477	0.4280	13.8

Fig. 5 shows the amplitude spectra calculated for the quasi-linear case and without lateral friction of the time series recorded at all 8 points in the basin area (see Fig. 2) for both wind directions. The amplitudes and phases of the 3 principal seiche modes derived from the spectra are shown in Tab. 1 (W 8 m s^{-1} wind) and in Tab. 2 (S 8 m s^{-1} wind).

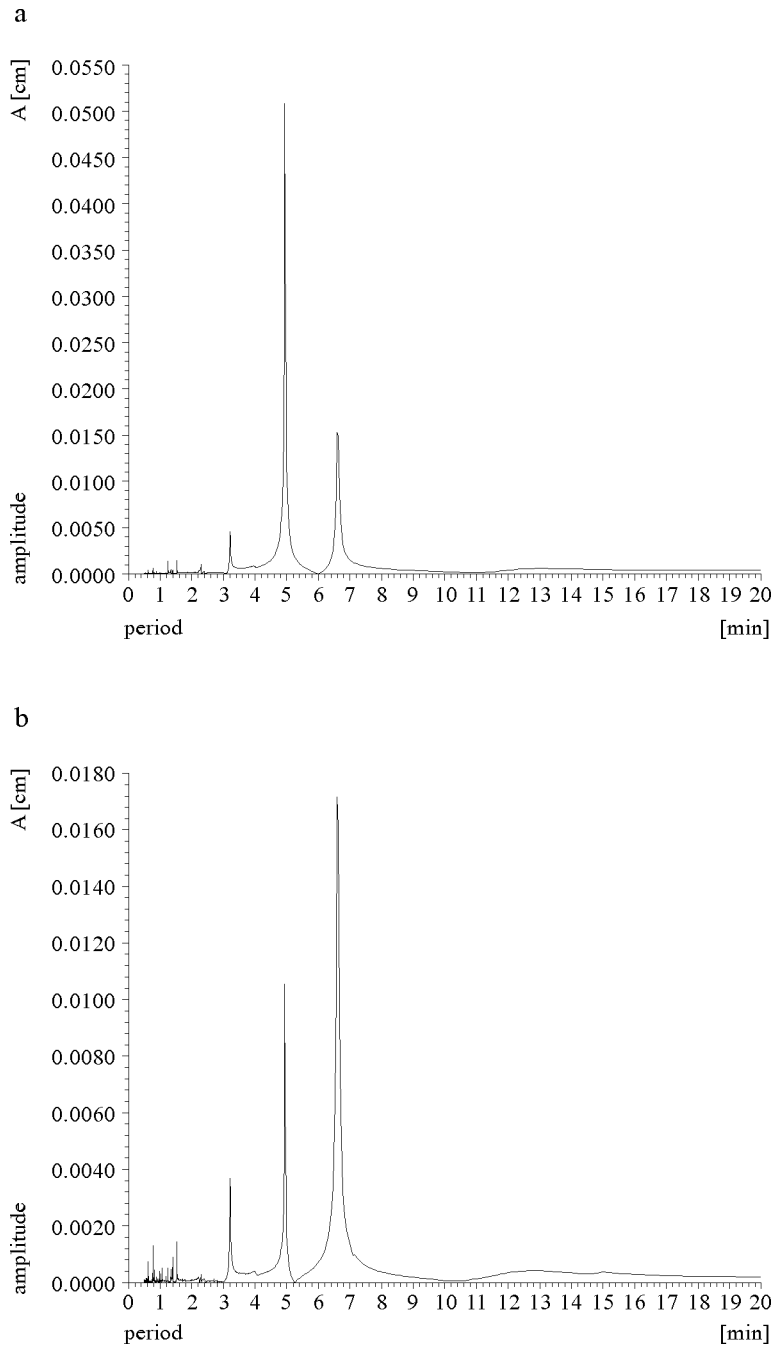

Fig. 4. Examples of amplitude spectra estimated with the aid of the discrete Fourier transformation for time series of sea level fluctuations at point 1 (for point location – see Fig. 2) in the case of W 8 m s^{-1} (a) and S 8 m s^{-1} (b) winds for the quasi-linear case without lateral friction ($A_l = 0$ cm^2 s^{-1})

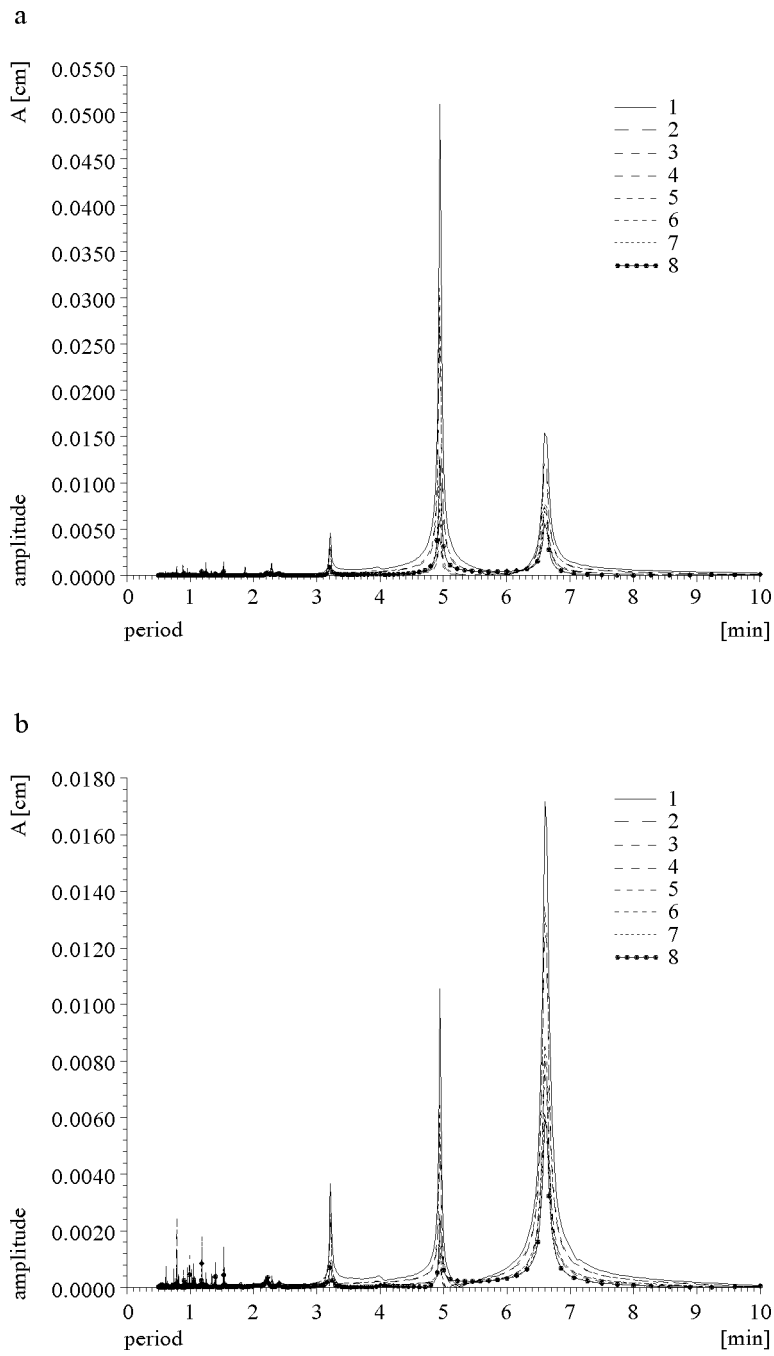

Fig. 5. Amplitude spectra estimated with the aid of the discrete Fourier transformation for time series of sea level fluctuations at 8 points (for point location – see Fig. 2) in the case of W 8 m s^{-1} (a) and S 8 m s^{-1} (b) winds for the quasi-linear case without lateral friction ($A_l = 0$ cm^2 s^{-1})

Table 2. Values of amplitudes and phases of the main seiches at 8 selected points estimated by the model for the case of a S 8 m s^{-1} wind when the lateral eddy exchange coefficient $A_l = 0$ cm^2 s^{-1} (quasi-linear case). Location of points – see Fig. 2

Point number	Seiche period [min]	Amplitude A_n [cm]	Relative amplitude A_n / A_{max}	Phase [grad]
1	3.2086	0.003684	0.2144	153.0
	4.9383	0.010551	0.6142	6.1
	6.5934	0.017179	1.0000	9.9
2	3.2000	0.000308	0.0240	28.8
	4.9383	0.005793	0.4515	6.6
	6.5934	0.012831	1.0000	10.0
3	3.2086	0.002490	0.3057	336.7
	4.9383	0.001321	0.1621	10.1
	6.5934	0.008145	1.0000	10.3
4	3.2086	0.002616	0.3424	336.7
	4.9383	0.000955	0.1250	12.0
	6.5934	0.007639	1.0000	10.4
5	3.2172	0.000251	0.0187	95.1
	4.9383	0.006436	0.4784	6.5
	6.5934	0.013454	1.0000	10.2
6	3.2086	0.002395	0.2789	336.7
	4.9383	0.001647	0.1918	9.3
	6.5934	0.008587	1.0000	10.4
7	3.2086	0.000995	0.1620	338.0
	4.9383	0.002537	0.4131	182.0
	6.5934	0.006140	1.0000	11.3
8	3.2086	0.000883	0.1476	338.1
	4.9383	0.002593	0.4336	182.1
	6.5934	0.005980	1.0000	11.5

In order to investigate the influence of the horizontal friction on the calculated seiche periods, we performed some experiments for selected values of the lateral eddy viscosity coefficient A_l. Fig. 6 depicts the results of the estimates of the amplitude spectra for time series of sea level variations at point 1 calculated by the quasi-linear model for both wind directions with different values of the lateral eddy viscosity coefficient: $A_l = 0$ cm^2 s^{-1}; 10^1 cm^2 s^{-1}; 10^2 cm^2 s^{-1}; 10^3 cm^2 s^{-1} and 10^4 cm^2 s^{-1} respectively. The amplitudes and phases of the three main seiche modes derived from the spectra estimated for the different values of the lateral eddy viscosity

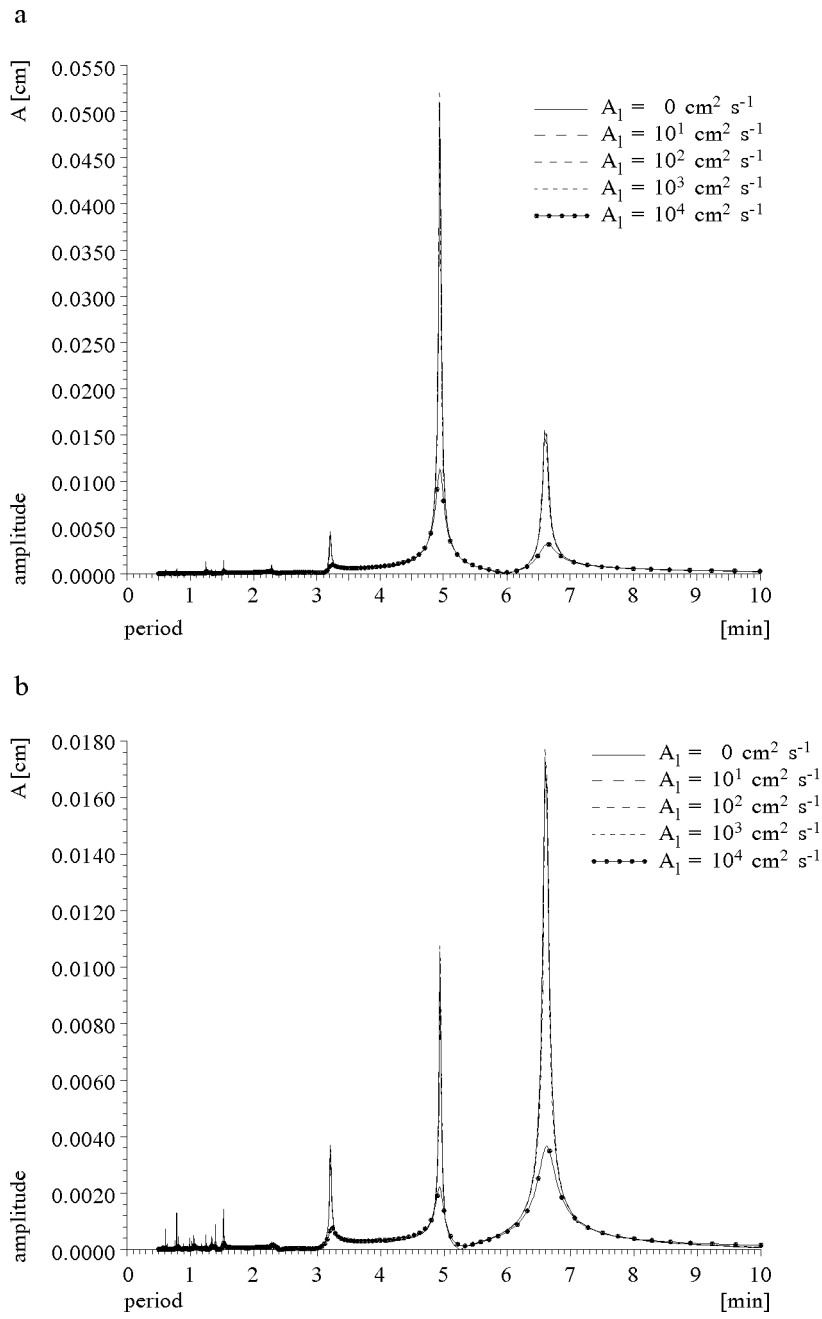

Fig. 6. Amplitude spectra estimated with the aid of the discrete Fourier transformation for time series of sea level fluctuations at point 1 (for point location – see Fig. 2) in the case of W 8 m s^{-1} (a) and S 8 m s^{-1} (b) winds for the quasi-linear case for different values of the lateral eddy viscosity coefficent A_l: 0, 10^1, 10^2, 10^3, 10^4 [cm^2 s^{-1}]

Table 3. Values of amplitudes and phases of the main seiches at point 1 estimated by the model for the case of a W 8 m s^{-1} wind for selected values of the lateral eddy exchange coefficient A_l (quasi-linear case)

A_l [cm^2 s^{-1}]	Period [min]	Amplitude A_n [cm]	Relative amplitude A_n / A_{max}	Phase [grad]
0	3.2086	0.004604	0.0905	145.7
	4.9383	0.050867	1.0000	357.4
	6.5934	0.015343	0.3016	10.3
10^1	3.2086	0.004610	0.0904	145.7
	4.9383	0.051013	1.0000	357.5
	6.5934	0.015388	0.3016	10.5
10^2	3.2086	0.004639	0.0893	145.6
	4.9383	0.051971	1.0000	358.0
	6.5934	0.015727	0.3026	11.8
10^3	3.2086	0.003975	0.0828	145.2
	4.9383	0.048011	1.0000	358.2
	6.5934	0.014735	0.3069	13.1
10^4	3.2345	0.001040	0.0913	115.4
	4.9383	0.011388	1.0000	348.1
	6.6298	0.003266	0.2868	332.2

coefficient A_l are shown in Tab. 3 and in Tab. 4 for the W 8 m s^{-1} and S 8 m s^{-1} winds respectively.

It is clear from the above results that the fundamental seiche mode in the Kirrbucht area (a closed basin) has periods equal to *ca* 6.59 min (longitudinal mode) and 4.94 min (transverse mode). The inclusion of lateral friction causes a considerable change in the periods of the main modes only when $A_l \geq 10^4$ cm^2 s^{-1}.

The crude estimates of the lateral eddy coefficient using eq. (11) for the basin area parameters are as follows:

- for $l \sim 20$ m (the smallest space-grid scale along the x-axis $\sim 2h_x$) gives $A_l \sim 2.5 \times 10^2$ cm^2 s^{-1};
- for $l \sim 100$ m ($\sim 10h_x$) gives $A_l \sim 2.2 \times 10^3$ cm^2 s^{-1}.

The above generally confirms the results of the investigations into the influence of lateral friction on the seiche mode characteristics.

The following numerical experiments were carried out to investigate the role of the non-linear terms in equations of motion (3)–(5) (the terms underlined once). The calculations were performed in the same manner as

Table 4. Values of amplitudes and phases of the main seiches at point 1 estimated by the model for the case of a S 8 m s^{-1} wind for selected values of the lateral eddy exchange coefficient A_l (quasi-linear case)

A_l [cm^2 s^{-1}]	Period [min]	Amplitude A_n [cm]	Relative amplitude A_n / A_{max}	Phase [grad]
0	3.2086	0.003684	0.2144	153.0
	4.9383	0.010551	0.6142	6.1
	6.5934	0.017179	1.0000	9.9
10^1	3.2086	0.003687	0.2139	153.0
	4.9383	0.010580	0.6137	6.2
	6.5934	0.017238	1.0000	10.0
10^2	3.2086	0.003712	0.2097	153.1
	4.9383	0.010759	0.6078	6.8
	6.5934	0.017702	1.0000	11.4
10^3	3.2086	0.003187	0.1844	153.2
	4.9383	0.009214	0.5333	6.2
	6.5934	0.017279	1.0000	14.4
10^4	3.2258	0.000784	0.2139	134.0
	4.9383	0.002226	0.6070	359.8
	6.6298	0.003668	1.0000	339.5

in the quasi-linear case for both wind directions and for selected values of the coefficient A_l. In this case, the perturbations due to the irregularities in the bottom relief and of the shoreline allowed a stable periodical numerical solution for a long calculation time (far longer than 20 h) to be obtained only when the lateral friction coefficient was $> 10^2$ cm^2 s^{-1}. Thus for comparison with the results for the quasi-linear case, the results of the present calculations are given here for two values of A_l (10^3 cm^2 s^{-1} and 10^4 cm^2 s^{-1}).

Fig. 7 presents the amplitude spectra calculated for the non-linear case and with the lateral friction coefficient $A_l = 10^3$ cm^2 s^{-1} of the time series recorded at all 8 selected points in the basin area (location of points – see Fig. 2) for both wind directions. The amplitudes and phases of the three principal seiche modes derived from the spectra are presented in Tab. 5 (W 8 m s^{-1} wind) and in Tab. 6 (S 8 m s^{-1} wind).

Fig. 8 depicts the estimated amplitude spectra for the time series of sea level variations at point 1 calculated for the non-linear case for both wind directions with two values of the lateral eddy viscosity coefficient: A_l = 10^3 cm^2 s^{-1} and 10^4 cm^2 s^{-1} respectively. The amplitudes and phases of the main three seiche modes derived from the spectra estimated with

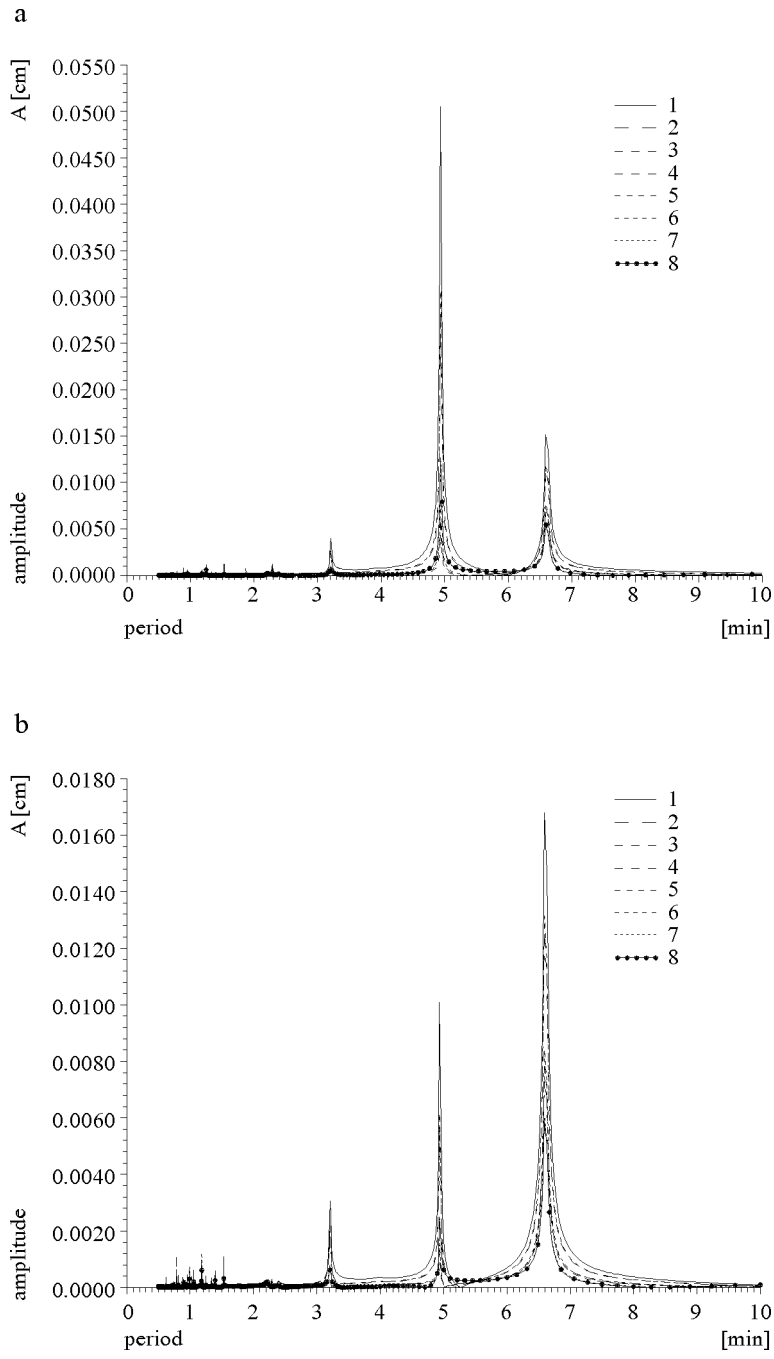

Fig. 7. Amplitude spectra estimated with the aid of the discrete Fourier transformation for time series of sea level fluctuations at 8 points (for point location – see Fig. 2) in the case of W 8 m s^{-1} (a) and S 8 m s^{-1} (b) winds for the non-linear case and a lateral friction coefficient of $A_l = 10^3$ cm^2 s^{-1}

Table 5. Values of amplitudes and phases of the main seiches at 8 selected points estimated by the model for the case of a W 8 m s^{-1} wind when the lateral eddy exchange coefficient $A_l = 10^3$ cm^2 s^{-1} (non-linear case). Location of points – see Fig. 2

Point number	Seiche period [min]	Amplitude A_n [cm]	Relative amplitude A_n / A_{max}	Phase [grad]
1	3.2086	0.004012	0.0794	141.0
	4.9383	0.050497	1.0000	356.0
	6.5934	0.015198	0.3010	11.8
2	3.2000	0.000455	0.0165	34.6
	4.9383	0.027628	1.0000	356.1
	6.5934	0.011393	0.4124	12.3
3	3.2086	0.002640	0.3623	328.1
	4.9383	0.006122	0.8400	357.3
	6.5934	0.007287	1.0000	13.4
4	3.2086	0.002772	0.4060	327.6
	4.9383	0.004316	0.6320	357.4
	6.5934	0.006829	1.0000	13.5
5	3.2172	0.000371	0.0121	83.5
	4.9383	0.030765	1.0000	356.2
	6.5934	0.011937	0.3880	12.3
6	3.2086	0.002542	0.3293	328.4
	4.9383	0.007721	1.0000	357.1
	6.5934	0.007676	0.9942	13.2
7	3.2086	0.001065	0.0860	326.2
	4.9383	0.012378	1.0000	174.7
	6.5934	0.005583	0.4511	14.4
8	3.2086	0.000943	0.0741	325.9
	4.9383	0.012719	1.0000	174.8
	6.5934	0.005444	0.4280	14.4

both values of the lateral eddy viscosity coefficient A_l are shown in Tabs. 7 and 8 for W 8 m s^{-1} and S 8 m s^{-1} winds respectively.

The results of the numerical calculations with the non-linear model confirmed the conclusions about the role of the lateral friction derived from the results of the quasi-linear case. The inclusion of non-linear terms did not alter the quasi-linear estimates of the main seiche periods.

The mode periods calculated using Merian's formulae (1) and (2) yield the following estimates of the periods of fundamental modes:

– for the mean depth of the basin estimated at 5 m, g = 9.80 m s^{-2};

– for horizontal characteristic lengths: L = 1350 m – 6.43 min and L = 1050 m – 5.0 min respectively.

These estimates are close to the findings based on the model calculations.

Table 6. Values of amplitudes and phases of the main seiches at 8 selected points estimated by the model for the case of a S 8 m s^{-1} wind when the lateral eddy exchange coefficient $A_l = 10^3$ cm^2 s^{-1} (non-linear case). Location of points – see Fig. 2

Point number	Seiche period [min]	Amplitude A_n [cm]	Relative amplitude A_n / A_{max}	Phase [grad]
1	3.2086	0.003072	0.1830	150.5
	4.9383	0.010098	0.6014	2.8
	6.5934	0.016791	1.0000	12.9
2	3.1667	0.017429	0.2873	119.6
	4.9383	0.005547	0.4422	3.2
	6.5934	0.012544	1.0000	13.0
3	3.2086	0.002067	0.2593	335.0
	4.9383	0.001259	0.1579	7.6
	6.5934	0.007972	1.0000	13.5
4	3.2086	0.002176	0.2913	335.0
	4.9383	0.000904	0.1210	9.8
	6.5934	0.007471	1.0000	13.5
5	3.2172	0.000217	0.0165	94.4
	4.9383	0.006162	0.4686	3.2
	6.5934	0.013151	1.0000	13.1
6	3.2086	0.001989	0.2368	335.1
	4.9383	0.001573	0.1873	6.8
	6.5934	0.008399	1.0000	13.5
7	3.2086	0.000822	0.1362	337.1
	4.9383	0.002436	0.4035	177.8
	6.5934	0.006037	1.0000	14.4
8	3.2086	0.000729	0.1240	337.6
	4.9383	0.002496	0.4246	177.9
	6.5934	0.005879	1.0000	14.5

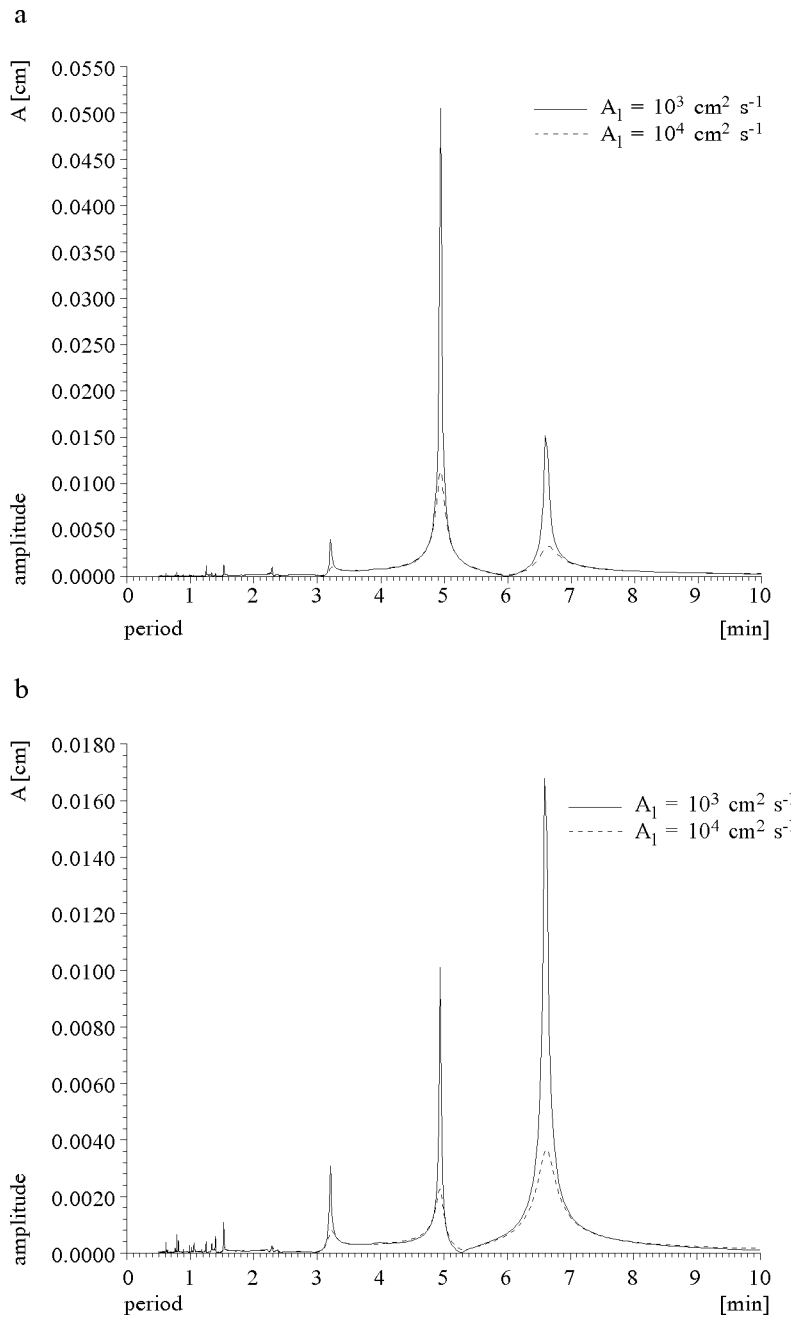

Fig. 8. Amplitude spectra estimated with the aid of the discrete Fourier transformation for time series of sea level fluctuations at point 1 (for point location – see Fig. 2) in the case of W 8 m s^{-1} (a) and S 8 m s^{-1} (b) winds for the non-linear case for different values of the lateral eddy viscosity coefficent A_l: 10^3, 10^4 [cm^2 s^{-1}]

Table 7. Values of amplitudes and phases of the main seiches at point 1 estimated by the model for the case of a W 8 m s^{-1} wind for selected values of the lateral eddy exchange coefficient A_l (non-linear case)

A_l [cm^2 s^{-1}]	Period [min]	Amplitude A_n [cm]	Relative amplitude A_n / A_{max}	Phase [grad]
10^3	3.2086	0.004012	0.0794	141.0
	4.9383	0.050497	1.0000	356.0
	6.5934	0.015198	0.3010	11.8
10^4	3.2345	0.001037	0.0908	116.4
	4.9383	0.011424	1.0000	347.8
	6.6298	0.003264	0.2857	332.3

Table 8. Values of amplitudes and phases of the main seiches at point 1 estimated by the model for the case of a S 8 m s^{-1} wind for selected values of the lateral eddy exchange coefficient A_l (non-linear case)

A_l [cm^2 s^{-1}]	Period [min]	Amplitude A_n [cm]	Relative amplitude A_n / A_{max}	Phase [grad]
10^3	3.2086	0.003072	0.1830	150.5
	4.9383	0.010098	0.6014	2.8
	6.5934	0.016791	1.0000	12.9
10^4	3.2258	0.000783	0.2138	134.9
	4.9383	0.002249	0.6142	358.5
	6.6298	0.003662	1.0000	339.5

4. Conclusions

The calculations of the periods of free sea level oscillations generated in the Kirrbucht during numerical simulations with the H–N model yielded the following results for two cases of wind direction with constant velocity 8 m s^{-1}:

- the fundamental longitudinal mode has a period equal to 6.59 min (y-direction),
- the fundamental transverse mode has a period equal to 4.94 min (x-direction),
- another significant mode of period equal to 3.21 min present in the amplitude spectra is probably a second-order longitudinal mode (y-axis, y-direction).

The inclusion of non-linear terms and lateral friction did not alter the periods; as expected, this merely changed the amplitudes of the seiches and their harmonic mode phases.

The results of the model calculations are believed to be verifiable of an estimation of the seiche parameters on the basis of planned *in situ* measurements of hydrological data. But in our opinion, the results in this paper provide some preliminary information on the time scales on which one can expect resonance phenomena in the Kirrbucht water dynamics in response to the impulse of a spatially homogeneous and temporally constant wind field.

Acknowledgements

The interest in the water dynamics of the Kirrbucht was awakened while Andrzej Jankowski was a visiting scientist at Rostock University in December 1995 and he wishes to express his gratitude to Rostock University for that invitation.

The numerical calculations were performed on the computers at the Institute of Oceanology of the Polish Academy of Sciences in Sopot and at the Academic Computer Centre in Gdańsk TASK, Poland.

References

Bendat J. S., Piersol A. G., 1986, *Random data. Analysis and measurement procedures*, 2nd ed., (revised and expanded), John Wiley a. Sons, New York–Chichester–Brisbane–Toronto–Singapore, 566 pp.

Defant A. I., 1961, *Physical oceanography*, 1, Pergamon Press, Oxford–London –Paris–New York, 729 pp.

Druet C., 1978, *Hydrodynamics of hydrotechnical constructions and harbour basins*, Wyd. Mor., Gdańsk, 390 pp., (in Polish).

Fairbridge R. W. (ed.), 1966, *Seiche*, [in:] *The Encyclopedia of oceanography*, 1, Reinhold Publ. Corporation, New York, 804–817.

Hansen W., 1962, *Hydrodynamical methods applied to oceanographic problems*, Proc. Symp. Math.–Hydrodyn. Meth. Phys. Oceanogr., Mitt. Inst. Meeresk. Hamburg Univ., 1, 25–34.

Hollan E., 1983, *Experiences with mathematical simulation of large scale motion in Lake Constance*, Mitt. Inst. Meeresk. Hamburg Univ., 26, 154–198.

Jankowski A., 1988, *Mathematical modelling of water circulation in the Baltic Sea*, Ossolineum, Wrocław, 281 pp., (in Polish).

Krauss W., 1973, *Dynamics of the homogeneous and the quasihomogeneous Ocean*, Gebrüder Borntraeger, Berlin–Stuttgart, 302 pp.

Kowalik Z., Murty T. S., 1993, *Numerical modelling of ocean dynamics*, Advanced Ser. on Ocean Eng., 5, World Sc., Singapore–New Jersey–London–Hong Kong, 481 pp.

Lewandowicz R., Staśkiewicz A., 1983, *Studies of free oscillations of the Little Puck Bay using numerical model*, Stud. i Mater. Oceanol., 40, 309–320, (in Polish).

Ozmidov R. V., 1968, *Horizontal turbulence and turbulent exchange in the ocean*, Nauka, Moskva, 200 pp., (in Russian).

Proudman J., 1953, *Dynamical oceanography*, Methuen Publ., London, 409 pp.

Ramming H. G., Kowalik Z., 1980, *Numerical modelling of marine hydrodynamics*, Elsevier, Amsterdam–Oxford–New York, 369 pp.

Simons T. J., 1973, *Development of three – dimensional numerical models of the Great Lakes*, Inland Water Directoriate Sc. Ser., 12, Canada Centre for Inland Waters, Burlington, 26 pp.

Appendix

Method of numerical solution of mass transport and sea level equations

The explicit numerical scheme of the Hansen Hydrodynamic-Numerical Method (Hansen, 1962) was used (see also Ramming and Kowalik, 1980). The finite difference form of the mass transport eqs. (3)–(5) can be written as follows (Ramming and Kowalik, 1980; Kowalik and Murty, 1993):

$$\begin{aligned} M_{x_{m+1,n}}^{t+\tau} &= (1-2R\tau)M_{x_{m+1,n}}^{t-\tau} + 2f\tau\overline{M_y} + 2\tau G_{x_{m+1,n}} + \\ &- \rho_0 g H_{m+1,n}\frac{\tau}{h_x}\left(\zeta_{m+2,n}^{t} - \zeta_{m,n}^{t}\right) + \\ &+ A_l\frac{\tau}{2h_x^2}\left(M_{x_{m+1,n+2}}^{t-\tau} + M_{x_{m+1,n-2}}^{t-\tau} + \right. \\ &+ \left. M_{x_{m+3,n}}^{t-\tau} + M_{x_{m-1,n}}^{t-\tau} - 4M_{x_{m+1,n}}^{t-\tau}\right) + \\ &- \frac{\tau}{h_x}\left(\frac{UPUX \times UPUX}{H} - \frac{UTUX \times UTUX}{H}\right) + \\ &+ \frac{\tau}{h_y}\left(\frac{VPUY \times UPUY}{H} - \frac{VTUY \times UTUY}{H}\right), \end{aligned} \tag{12}$$

$$\begin{aligned} M_{y_{m,n+1}}^{t+\tau} &= (1-2R\tau)M_{y_{m,n+1}}^{t-\tau} - 2f\tau\overline{M_x} + 2\tau G_{y_{m,n+1}} + \\ &- \rho_0 g H_{m,n+1}\frac{\tau}{h_y}\left(\zeta_{m,n+2}^{t} - \zeta_{m,n}^{t}\right) + \\ &+ A_l\frac{\tau}{2h_y^2}\left(M_{y_{m+2,n+1}}^{t-\tau} + M_{y_{m-2,n+1}}^{t-\tau} + \right. \\ &+ \left. M_{y_{m,n+3}}^{t-\tau} + M_{y_{m,n-1}}^{t-\tau} - 4M_{y_{m,n+1}}^{t-\tau}\right) + \\ &- \frac{\tau}{h_x}\left(\frac{UPVX \times VPVX}{H} - \frac{UTVX \times VTVX}{H}\right) + \\ &+ \frac{\tau}{h_y}\left(\frac{VPVY \times VPVY}{H} - \frac{VTVY \times VTVY}{H}\right), \end{aligned} \tag{13}$$

$$\begin{aligned} \zeta_{m,n}^{t+2\tau} &= \zeta_{m,n}^{t} - \frac{\tau}{\rho_0}\left(\frac{1}{h_x}(M_{x_{m+1,n}}^{t+\tau} - M_{x_{m-1,n}}^{t+\tau}) + \right. \\ &+ \left. \frac{1}{h_y}(M_{y_{m,n+1}}^{t+\tau} - M_{y_{m,n-1}}^{t+\tau})\right), \end{aligned} \tag{14}$$

where

$$G_{x_{m+1,n}} = H_{m+1,n}\frac{(p_{a_{m+2,n}} - p_{a_{m,n}})}{2h_x} + \tau^s_{x_{m+1,n}}, \tag{15}$$

$$G_{y_{m,n+1}} = H_{m,n+1}\frac{(p_{a_{m,n+2}} - p_{a_{m,n}})}{2h_y} + \tau^s_{y_{m,n+1}}, \tag{16}$$

$$\overline{M_y} = 0.25(M^{t-\tau}_{y_{m+2,n+1}} + M^{t-\tau}_{y_{m+2,n-1}} + M^{t-\tau}_{y_{m,n+1}} + M^{t-\tau}_{y_{m,n-1}}), \tag{17}$$

$$\overline{M_x} = 0.25(M^{t-\tau}_{x_{m+1,n+2}} + M^{t-\tau}_{x_{m-1,n+2}} + M^{t-\tau}_{x_{m+1,n}} + M^{t-\tau}_{x_{m-1,n}}), \tag{18}$$

$$\begin{aligned}
UPUX &= 0.5 \times (M^{t-\tau}_{x_{m+1,n}} + M^{t-\tau}_{x_{m+3,n}}),\\
UTUX &= 0.5 \times (M^{t-\tau}_{x_{m+1,n}} + M^{t-\tau}_{x_{m-1,n}}),\\
VPUY &= 0.5 \times (M^{t-\tau}_{y_{m+2,n+1}} + M^{t-\tau}_{y_{m,n+1}}),\\
UPUY &= 0.5 \times (M^{t-\tau}_{x_{m+1,n}} + M^{t-\tau}_{x_{m+1,n+2}}),\\
VTUY &= 0.5 \times (M^{t-\tau}_{y_{m+2,n-1}} + M^{t-\tau}_{y_{m,n-1}}),\\
UTUY &= 0.5 \times (M^{t-\tau}_{x_{m+1,n}} + M^{t-\tau}_{x_{m+1,n-2}}),\\
UPVX &= 0.5 \times (M^{t-\tau}_{x_{m+3,n}} + M^{t-\tau}_{x_{m+3,n-2}}),\\
VPVX &= 0.5 \times (M^{t-\tau}_{y_{m,n+1}} + M^{t-\tau}_{y_{m+2,n+1}}),\\
UTVX &= 0.5 \times (M^{t-\tau}_{x_{m+1,n}} + M^{t-\tau}_{x_{m+1,n-2}}),\\
VTVX &= 0.5 \times (M^{t-\tau}_{y_{m,n+1}} + M^{t-\tau}_{y_{m-2,n+1}}),\\
VPVY &= 0.5 \times (M^{t-\tau}_{y_{m,n+1}} + M^{t-\tau}_{y_{m,n+3}}),\\
VTVY &= 0.5 \times (M^{t-\tau}_{y_{m,n+1}} + M^{t-\tau}_{y_{m,n-1}}).
\end{aligned}$$

The stability condition for the above finite difference scheme are as follows (this is similar to the standard CFL criterion) (Ramming and Kowalik, 1980; Kowalik and Murty, 1993):

$$\tau \leq \frac{h}{\sqrt{2gH_{\max}}}, \tag{19}$$

where

$H_{\max}$ – maximal basin depth,
τ – time step,
h – space step: $h = \max(h_x, h_y)$,
h_x, h_y – space steps of the H–N numerical grid along axes OX and OY respectively.